Hindawi
Journal of Nanomaterials
Volume 2021, Article ID 4449890, 9 pages
https://doi.org/10.1155/2021/4449890

Research Article

Effect of Deposition Conditions on Phase Content and Mechanical Properties of Yttria-Stabilized Zirconia Thin Films Deposited by Sol-Gel/Dip-Coating

Francisco J. Cano,[1] Orlando Castilleja-Escobedo,[1] L. J. Espinoza-Pérez,[1,2] Cecilia Reynosa-Martínez,[1] and Eddie Lopez-Honorato [1,3]

[1]*Centro de Investigación y de Estudios Avanzados del IPN (CINVESTAV), Avenida Industria Metalúrgica 1062, Ramos Arizpe, Coahuila 25900, Mexico*
[2]*Universidad Nacional de Ingenieria (UNI), Sede Central, Avenida Universitaria, 5595 Managua, Nicaragua*
[3]*Oak Ridge National Laboratory, Oak Ridge, TN 37831, USA*

Correspondence should be addressed to Eddie Lopez-Honorato; honoratole@ornl.gov

Received 11 May 2021; Revised 16 September 2021; Accepted 27 September 2021; Published 13 October 2021

Academic Editor: Domenico Acierno

The effect of yttria concentration (0-33.4 mol%), extraction rates (0.17, 0.33, 0.50, and 0.67 mm s^{-1}), and the number of layers (up to four) on the phase content, surface defects, thickness, hardness, adhesion strength, and wear rate of yttria-stabilized zirconia coatings produced by sol-gel/dip-coating were studied for its use on thermolabile substrates. At 700°C, a metastable tetragonal phase (t'') was obtained even with 33.4 mol% yttria when heat treated for 24 hours; however, a fully cubic structure was attained by extending the heat treatment up to 48 hours as confirmed by Raman spectroscopy. Furthermore, it was necessary to use withdrawal speeds of at least 0.67 mm s^{-1} to produce defect-free coatings. Although the coatings were produced at low temperature, they showed 41% lower wear rate than steel and an adhesion strength of 30 MPa. Our work stresses the importance of the heat treatment history on the stabilization of the cubic phase in sol-gel YSZ coatings.

1. Introduction

Yttria-stabilized zirconia (YSZ) due to its low thermal conductivity, chemical inertness, radiation resistance, and high mechanical properties has been proposed for a wide range of applications in the nuclear industry, such as inert matrix fuel, diffusion barrier to avoid fuel-matrix interaction, sacrificial coatings, and thermal insulator, among others [1–6]. However, some of these applications require the deposition of YSZ at low temperatures (for example, 1050°C on T91 steel or 800°C on Ni alloys) to avoid phase changes or considerable reductions on mechanical properties on thermolabile substrates [3, 7, 8]. In addition to this requirement, for nuclear applications, the production of YSZ with a fully cubic structure is also desirable to increase its tolerance to neutron irradiation [9–12].

Overall, among the different deposition techniques available to deposit YSZ, sol-gel/dip-coating is comparatively simple, cost-effective, and capable of producing coatings at low temperatures [13]. However, a common feature associated with the deposition of YSZ thin films and coatings through sol-gel/dip-coating is the production of materials with cracks or defects if the heat treatment or deposition conditions are not controlled [3, 14–16]. For example, it has been observed that coatings thicker than 200 nm are prone to cracking due to the release of gases, thermal mismatch between the coating and the substrate, and internal stresses during heat treatment [17–19]. Crack formation can be reduced or avoided by controlling the sol-gel fabrication route (for example, using complexing agents affecting the hydrolysis and condensation reactions or by modifying the viscosity of the gel), the extraction rate, and heat

treatment temperature or by depositing several consecutive coatings for the purpose of filling the cracks that are generated [14, 16, 19–21]. Higher heat treatment temperatures tend to reduce the formation of cracks, whereas the deposition of a multilayer system can result in coatings with lower wear life and reduced performance at high temperature due to a weak bonding between each film [22, 23]. Furthermore, some reports have shown that the cubic phase, needed for nuclear applications, is not favorable below 800°C, resulting in the formation of a tetragonal phase even with 18.2 mol% yttria at 1150°C due to the limited diffusion at those low temperatures [16, 21, 24]. Therefore, it is important to study the production of YSZ at low temperatures to obtain defect free, fully cubic, and mechanical resistant structures.

This work describes the production of YSZ thin films at 700°C, showing that the tetragonal phase (t' and t'') was maintained even with concentration up to 33.4 mol% yttria after 24 h of sintering. A fully cubic structure was achieved only after 48 hours of heat treatment with 29.0 and 33.4 mol% yttria, as confirmed by X-ray diffraction (XRD) and Raman spectroscopy. Additionally, it was feasible to produce defect-free film layers up to 824 nm thick by controlling the extraction rate during dip-coating. Finally, contrary to previous reports, we show that a multilayer YSZ coating system sintered at 700°C produced an increase in hardness and wear resistance of 93 and 42% compared to steel, respectively, by maintaining an adhesion strength of 30 MPa.

2. Materials and Methods

Yttria-stabilized zirconia (YSZ) coatings were deposited on $2 \times 1\,cm^2$ stainless steel 304 substrates. These substrates were ground with abrasive SiC paper and then polished with 3 and 1 μm diamond paste. Finally, the samples were immersed in an ultrasound bath with Citranox and then in an ethanol/acetone solution.

An initial solution was prepared by mixing 27.4 ml of zirconium n-propoxide (ZNP) (70% by weight in isopropanol, Sigma-Aldrich), 35.6 ml of ethanol (99.8%, Vetec), and 3.8 ml HNO_3 (6.3%, JT Baker) under argon atmosphere and constant stirring (300 rpm). After 6 hours, a mixture of 7.7 ml of distilled water and 2.7 ml of acetic acid (99.7%, Jalmek) (weight ratio 3 : 1) was added. The molar ratios used for these solutions were 10 : 1 for ethanol : ZNP, 6.6 : 1 for isopropanol : ZNP, and 7 : 1 for H_2O : ZNP. A second solution was prepared with 6.7 g of yttrium acetate (99.9%, Sigma-Aldrich), 9.2 ml of isopropanol (99.5%, from Jalmek), and 10 ml of HNO_3 (this last one added drop by drop until the solution became transparent), maintaining the solution stirred for 1 h at 300 rpm to obtain a 29 mol% of $YO_{1.5}$ (29YSZ). Similar solutions were prepared, this time modifying the amount of yttrium acetate in order to achieve a mol percentage of 7.6, 11.4, 14.8, 18.2, and 33.4% mol of $YO_{1.5}$.

The coatings were obtained using a dip-coater (WPTL6-0.01 MTI Corporation) by introducing the samples to the gel for 60 seconds and varying the extraction rates at 0.17, 0.33, 0.50, and 0.67 mm s^{-1}. After extraction, samples were dried in air at room temperature for 24 hours and then at 500°C for 2 hours (using a heating/cooling rate of 1°C/min). The previous procedure was repeated between each deposition in multilayered coatings (up to 4 layers) before the final heat treatment at 700°C in air for 24 or 48 h (using a heating/-cooling rate of 10°C/min). After this final heat treatment, the microstructure and mechanical properties of the coatings were characterized.

YSZ with 29.0 (29YSZ) and 33.4 mol% of yttria (33.4YSZ) were characterized by thermogravimetric analysis under air atmosphere, using a thermal analyzer instrument (TA Instruments, SDT Q600), with a heating rate of 10°C/min. The microstructure of the coatings was characterized by scanning electron microscopy (SEM), using a Philips XL30 microscope using an accelerating voltage of 20 kV. The composition was characterized by energy-dispersive X-ray spectroscopy (EDS). The phase content of YSZ powders obtained after the heat treatment of the solutions was characterized by X-ray diffraction (XRD) (PANalytical Empyrean) in the regions $10° \le 2\theta \le 80°$ and $71° \le 2\theta \le 76°$, using a step size of 0.03° and 3 s per step, with a CuKα radiation of 1.542 Å wavelength. The crystallite size was calculated from the (111) plane at 30° using the Scherrer formula.

$$D(\text{nm}) = \frac{0.89\lambda}{\text{FWHM}\,\text{Cos}\theta}, \tag{1}$$

where D is the crystallite size in nm, λ the X-ray wavelength, FWHM the full-width at half maximum of the diffraction peak, and θ the diffraction-peak angle. The lattice parameters (c and a) were obtained using the software MDI Jade 6. The tetragonality factor ($c/\sqrt{2}a$) was used to identify the metastable tetragonal (t' and t'') or cubic phases [24, 25]. Additionally, Raman spectroscopy (Renishaw inVia) was also used to characterize the phase content using a 514 nm wavelength laser, and a 50x lens obtaining a spot size of approximately 5 μm.

The thickness of each layer was measured by profilometry using a KLA Tencor D-600 profilometer. The hardness of the coatings was evaluated by indentation using the ASTM C1327-08 Norm, using Shimadzu G21 series equipment with a Vickers indenter and applying a load of 25 grams-force. The adhesion strength was determined by Pull-Off tests based on the ASTM D4541-09 method using a universal testing machine MTS QTest/100 equipment. Finally, abrasion resistance was determined using a Pin-on-Disk Tribometer (Microtest MT Series), using the ASTM G99-95a method, with a load of 10 N, a ball of steel Al-chrome of 4 mm diameter, a distance of 20 m, and a speed of 30 rpm.

3. Results and Discussion

3.1. Effect of Yttria Concentration and Sintering Time. Figure 1 shows the thermogravimetric analysis of YSZ produced with 29 mol% yttria (29YSZ). Overall, three different stages in the transformation of YSZ were observed. In stage I, which ranged from room temperature up to approximately 220°C, a weight loss of ~15% was observed. This weight loss has been associated with the vaporization of superficial and structural water [19, 25–28]. The stage II,

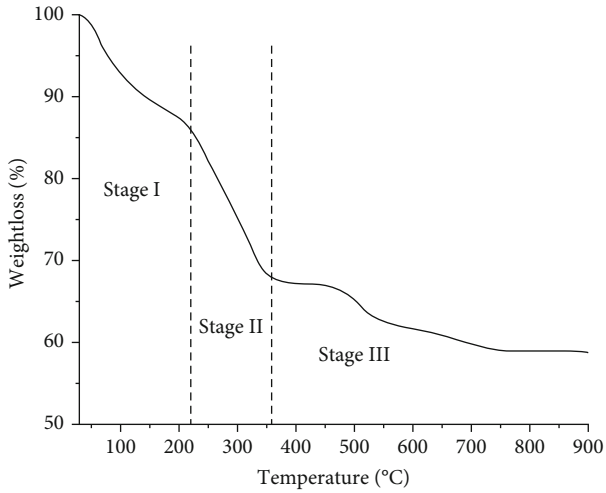

Figure 1: TGA curve of YSZ with 29 mol% $YO_{1.5}$ (29YSZ).

which ranges from 220 to 350°C, with a weight loss of 19%, has been associated with the combustion and decomposition of organic compounds [19, 26, 28–30]. The stage III, above 350°C, accompanied by a final weight loss of 10%, has been correlated with the decomposition of nitrates originated from the nitric acid [29], as well as the beginning of the crystallization of YSZ [30]. A similar behavior was observed for YSZ with 33.4 mol% yttria (33.4YSZ) in Figure S1 (supplementary material).

Figure 2 shows the X-ray diffraction patterns obtained for the zirconia powders doped with different yttria concentration (0–33.4 mol% $YO_{1.5}$) and heat treated at 700°C for 24 h. The zirconia synthesized without any dopant (0YSZ) showed the characteristic reflections of both the monoclinic (m) and tetragonal (t) phases. On the other hand, zirconia powders doped with 7.6–33.4 mol% $YO_{1.5}$ showed the reflection characteristic of the tetragonal (t) and/or cubic (c) phase. Moreover, Table 1 shows that, at 700°C, the increase in the molar content of $YO_{1.5}$ from 7.6 to 33.4 caused a decrease in the crystallite size from 13.2 to 6.1 nm, respectively, i.e., the crystal growth was inhibited by the increase in the yttria content. This behavior has been correlated to the segregation of yttria at the grain boundaries, decreasing the mass transfer by surface diffusion and avoiding the crystal growth [31, 32]. Furthermore, it has been reported that higher concentrations of yttria change the crystallization temperature to higher values, retarding the crystal growth [33]. Similarly, inhibition of crystal growth has been reported in zirconia systems doped with aluminum and europium [34, 35]. The occurrence of the tetragonal zirconia at room temperature and without the use of any dopant in sample 0YSZ could due to the crystallite size, which is below the critical crystallite size of around 30 nm, below which the tetragonal phase can exist at low temperatures due to a larger specific surface area and an excess of energy [36].

Although generally the tetragonal phase could be differentiated from the cubic phase due to the presence of doublets in the diffraction pattern in angles below 70°, the broadening of the signals due to small crystallite sizes (see Table 1), particularly at low sintering temperatures, makes

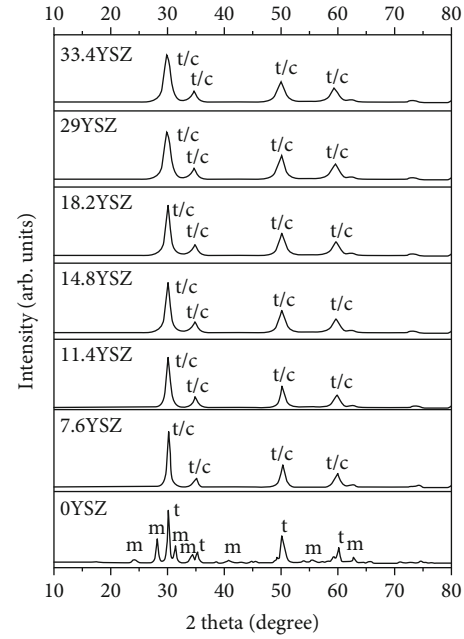

Figure 2: XRD patterns of zirconia powders doped with 0-33.4 mol% $YO_{1.5}$, heat treated at 700°C for 24 h, region $10° \leq 2\theta \leq 80°$.

this differentiation by simple observation unpractical [37, 38]. Therefore, a more detailed analysis was performed using the diffractograms between 71 and 76° (Figure 3) and the tetragonality factor $c/\sqrt{2}a$ in Table 1.

Figure 3 shows the diffraction patterns between 71 and 76°. The 7.6 mol% yttria powders had signals at 73° and 74.5°, which are characteristics of the tetragonal phase [37], whereas at 11.4 mol%, an asymmetric diffraction pattern centered at 74° was observed, likely due to a mixture of tetragonal and cubic/metastable tetragonal phase (t'') [37]. Above 18.2 mol% yttria, the diffraction patterns could suggest the formation of a fully cubic structure. However, Yashima et al. have suggested the existence of a metastable tetragonal phase t'', which differentiates from the cubic phase due to a slight distortion of the anionic network [24, 38]. The presence of the tetragonal (transformable, nontransformable, and metastable: t, t', and t'', respectively) or cubic phases could be differentiated based on their tetragonality, where a tetragonality of 1 would suggest a cubic or t'' phase [24, 25].

Table 1 shows that the tetragonality decreased from 1.0059 to 1.0000 as the molar concentration of yttria increased from 7.6 to 33.4 mol% [24, 38, 39]. According to the relationship between tetragonality and phase content suggested by Viazzi et al. [38], zirconia powders with yttria contents between 7.6 and 18.2 mol% developed a nontransformable tetragonal phase (t'), while the tetragonal metastable (t'') or cubic phase (c) could be assigned to zirconia powders with an yttria content between 29 and 33.4 mol% [38].

Raman spectroscopy was used to further characterize the YSZ produced since Raman spectroscopy is highly sensitive to phase transitions induced by oxygen displacement, even without a long-range periodicity [40, 41]. Figure 4 shows

Table 1: Crystallite size, lattice parameters, and tetragonality factor for zirconia powders doped with 7.6-33.4 mol% yttria, heat treated at 700°C for 24 h.

Nomenclature	$YO_{1.5}$ content (mol%)	Crystallite size (nm)	a (Å)	c (Å)	$c/\sqrt{2}a$	Phase
7.6YSZ	7.6	13.2	3.6181	5.1471	1.0059	t'
11.4YSZ	11.4	10.1	3.6288	5.1398	1.0015	t'
14.8YSZ	14.8	8.9	3.6306	5.1389	1.0009	t'
18.2YSZ	18.2	7.5	3.6366	5.1456	1.0005	t'
29YSZ	29.0	6.4	3.6392	5.1464	1.0000	t''/c
33.4YSZ	33.4	6.1	3.6540	5.1530	1.0000	t''/c

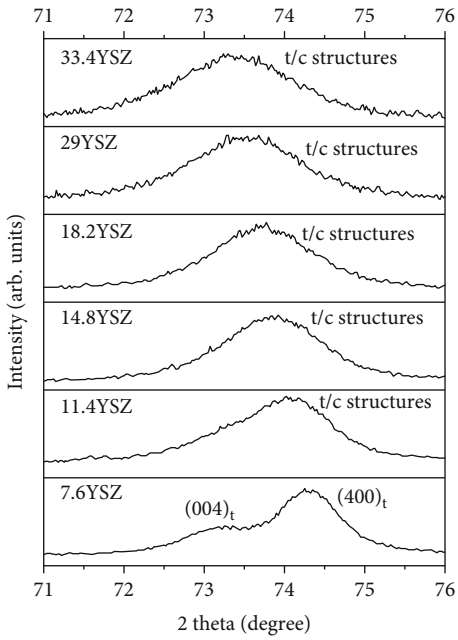

Figure 3: XRD patterns of zirconia powders doped with 7.6-33.4 mol% $YO_{1.5}$, heat treated at 700°C for 24 h, region $71° \leq 2\theta \leq 76°$.

the Raman spectra of 29 and 33.4 mol% yttria heat treated at 700°C for 24 and 48 h. As can be seen in Figure 4(a), the Raman spectra of zirconia powders with 29 mol% yttria (29YSZ) showed five bands located at 146, 261, 319, 465, and 639 cm^{-1}, corresponding to the tetragonal zirconia [42]. On the other hand, the Raman spectrum of zirconia powder doped with 33.4 mol% yttria (33.4YSZ) showed an additional broad and intense band at 568 cm^{-1}, which corresponds to the cubic structure of zirconia [42]. This suggests that the YSZ with 29 and 33.4 mol% was indeed metastable tetragonal phase (t'') with possibly a mixture of cubic phase for 33.4 mol% yttria.

Considering that Yashima and coworkers [24] showed that extended sintering time could promote the stabilization of cubic phase, samples were heat treated up to 48 h. Figure 4(b) shows that the extended sintering time resulted in important changes in the Raman spectra compared to 24 h. For 29 and 33.4 mol% yttria, only 2 bands position at 141 and 590 cm^{-1} were identified, whose similar spectra have been assigned to the cubic phase [42]. This indicates that prolonged heat treatment promoted the diffusion of cations and stabilization of the cubic phase [24].

The phase diagram proposed by Yashima et al. [24] for metastable-stable phases of zirconia (Figure 5) suggests that among the samples produced between 7.6 and 18.2 mol% yttria should have resulted in a mixture of monoclinic+cubic phases ($m + c$) at 700°C. The presence of a tetragonal (t') phase instead of a monoclinic+cubic might be possible due to the very small crystallite size of 13.2, 10.1, 8.9, and 7.5 nm for 7.6, 11.4, 14.8, and 18.2 mol% yttria, whose values are below the 30 nm value necessary to stabilize this phase even without the presence of yttria [36].

In accordance with our results (for the samples with an extended sintering time), the phase diagram proposed by Yashima et al. predicts that concentrations at 29-33.4 mol % yttria should have produced a fully cubic structure. It has been proposed that the stabilization of these metastable phases is achieved by the energy barrier (stabilized by kinetics) rather than the free energy difference, as it takes a long time to achieve a stable phase. This was corroborated with the extended sintering time, which after 48 h, achieved the stabilization of the cubic phase (Figure 4(b)).

3.2. Microstructure and Thickness. It was observed that for coatings with a single deposition, the withdrawal speed did not affect the quality of the coating, since only homogeneous and translucent (only the microstructure of steel was observed) coatings were obtained for all speeds. Conversely, when two layers were deposited, defects were identified using a withdrawal speed of 0.17 mm s^{-1}. Nevertheless, it was possible to obtain defect-free coatings with only the steel microstructure visible, with 0.67 mm s^{-1}. A similar trend was observed when depositing four layers (Figures 6(a) and 6(b)), where homogeneous coatings were only deposited at 0.67 mm s^{-1} (Figure 6(b)). The formation of a dense and crack-free layer is relevant for its corrosion resistance since it is through the cracks or other defects where water or other corrosive elements can penetrate into the substrate [19, 43].

Figure 7 shows the thickness measured by profilometry for coatings with 33.4 mol% of yttria in the precursor solution. Overall, thicker layers were obtained with higher withdrawal speeds and the number of layers; for example, the initial coating thickness increased from 226 to 231, 258, and 285 nm as the withdrawal speed increased to 0.17,

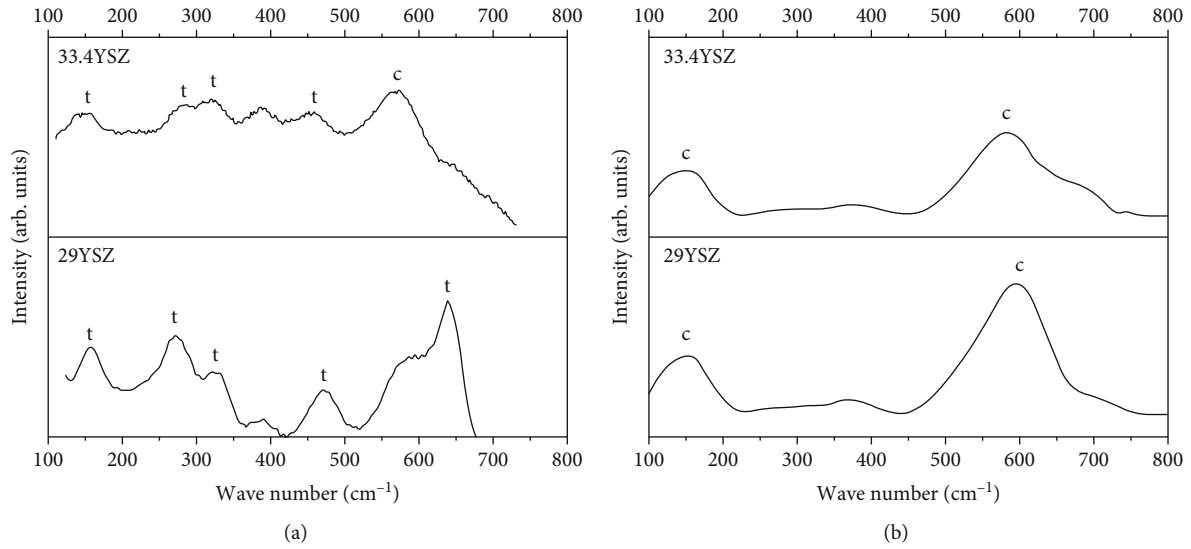

FIGURE 4: Raman spectra of zirconia powders doped with 29 and 33.4 mol% of yttria and heat treated at 700°C for (a) 24 h and (b) 48 h.

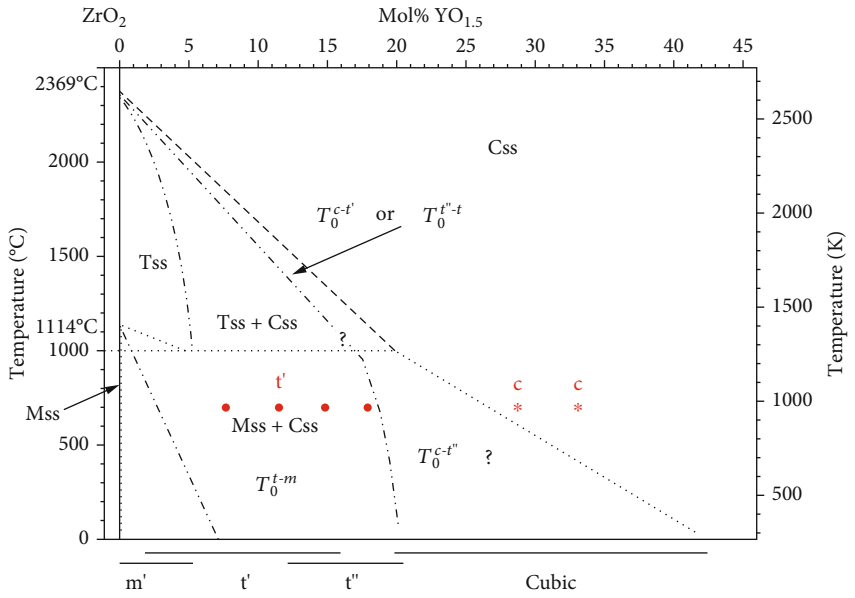

FIGURE 5: Modified metastable-stable phase diagram of the ZrO_2-rich portion in the ZrO_2-$YO_{1.5}$ system proposed by Yashima and coworkers [24]. Point mark shows the samples produced in this work. The star mark shows the samples sintered at 24 and 48 h. Only the samples sintered for 48 h produced a fully cubic structure. SS: solid solution; M or m: monoclinic phase; T or t: transformable tetragonal phase; C or c: cubic phase; t': nontransformable tetragonal phase; t'': metastable tetragonal phase.

0.33, 0.50, and 0.67 mm s^{-1}, respectively. Coating thickness changed from 226 up to 502 nm when depositing one and four layers, respectively, with a withdrawal speed of 0.17 mm s^{-1}. Similarly, the coating thickness changed from 285 to 824 nm with one and four layers, respectively, using a withdrawal speed of 0.67 mm s^{-1}.

The increase in a single-layer coating thickness of 59 nm with a withdrawal speed increase from 0.17 to 0.67 mm s^{-1} suggests that the deposition was performed most likely in the intermediate regime [44]. The overall thickness increased with more layers deposited; however, each layer produced a thinner coating. It is likely that the modification of the substrate with a previous YSZ thin film affected the wetting property and adhesion of the fluid on the substrate, as well as the capillary pressure, by modifying the surface tension and the rates of condensation and evaporation [45]. The thickness of the thin films deposited was higher than other reports that showed the production of 970 nm after 15 deposits using 1 mm/s [19] or 130 nm with 3 layers using 0.5 mm/s [43]. The main difference between these reports and the present work is the use of acetic acid instead of acetylacetone. The use of acetic acid tends to promote condensation reactions, in comparison to AcAc, which forms complexes with zirconium propoxide, which are more

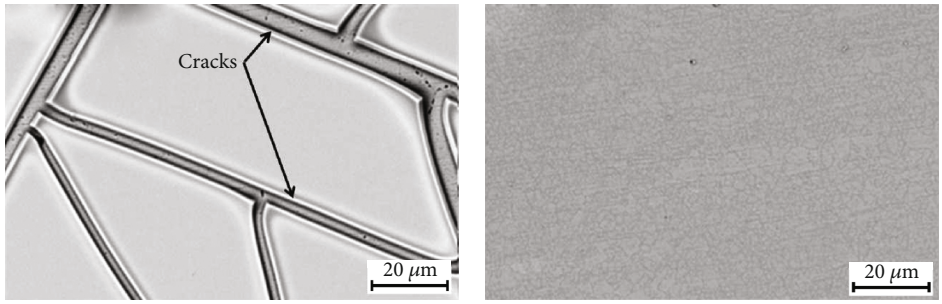

(a) (b)

Figure 6: YSZ thin films heat treated at 700°C for 24 h, with four layers deposited using a withdrawal speed of (a) 0.17 and (b) 0.67 mm s^{-1}.

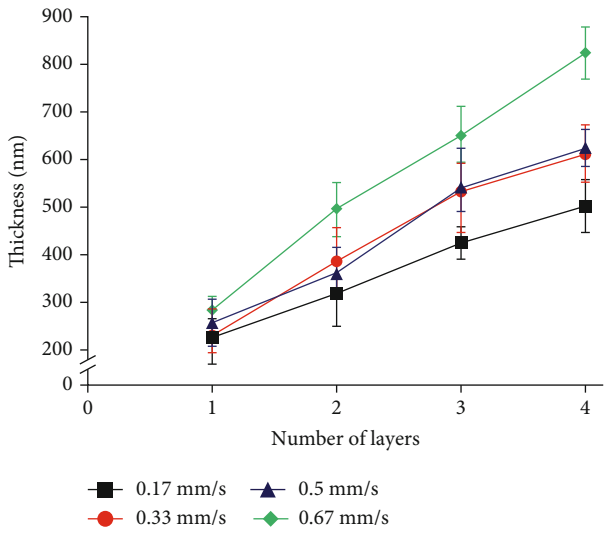

Figure 7: Coating thickness of 33.4YSZ films heat treated at 700°C for 24 h, measured by profilometry.

Table 2: Results of Pull-Off adhesion strength of 33.4YSZ films on steel (MPa).

Layers/extraction rates	0.17 mm/s	0.33 mm/s	0.5 mm/s	0.67 mm/s
1 layer	29.7 ± 0.5	29.8 ± 0.8	30.0 ± 0.5	29.5 ± 0.6
2 layers	29.7 ± 0.4	29.2 ± 0.6	29.0 ± 0.7	29.0 ± 0.5
3 layers	29.0 ± 0.5	30.2 ± 0.4	29.2 ± 0.8	30.2 ± 0.8
4 layers	29.6 ± 0.7	28.3 ± 0.6	28.0 ± 0.8	29.8 ± 0.7

difficult to hydrolize, also reducing the condensation process [29].

3.3. Mechanical Properties. The mechanical properties of the 33.4YSZ coatings produced were characterized. Table 2 shows the effect of coating layers and extraction rates on the adhesion strength. All samples showed an adherence strength between 28 and 30 MPa. These values are higher than those obtained by sol-gel YSZ on carbon steel (2.5–12.4 MPa) [17], as well as YSZ deposited by RF magnetron sputtering on 316 L stainless steel (12–26 MPa) [46]. The adhesion strength was even higher than some YSZ coatings

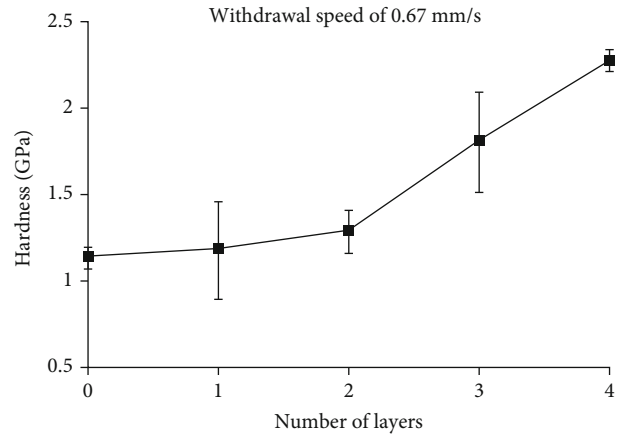

Figure 8: Effect of the number of YSZ layers on the hardness of 33.4YSZ/steel, films heat treated at 700°C for 24 h.

produced by plasma spray, which reported values between 15 and 30 MPa [47–49].

The good adherence of the coatings produced at low temperatures has been attributed to a condensation reaction between the alkoxide molecule and the hydroxyl groups on the surface of the metal, resulting in a Zr-O-Fe bond [50]. However, thermogravimetric analysis (TGA) results suggested that at 700°C, these molecules were already removed, making them an unlikely route of adhesion (Figure 1). Conversely, previous reports have suggested a partial diffusion of Fe, Cr, and Ni into YSZ at the YSZ/steel interface [20, 43, 50]. Therefore, the good adhesion of up to 30 MPa observed in this study could be the result of the prolonged heat treatment (48 hours) at 700°C, compared with the shorter isotherms generally used during sintering of YSZ coatings for around 1 to 2 hours [23, 26, 51].

The effect of the coatings on the hardness of the surface (a combination of the hardness of steel and the coating) was also evaluated for 33.4YSZ coatings deposited at 0.67 mm s^{-1} (Figure 8). Although nanoindentation would have been ideal to characterize these films (not available for this study), microindentation showed that the hardness of the surface increased with every layer deposited, reaching twice the hardness of steel from 1.18 up to 2.28 GPa for four YSZ layers.

The good adherence and mechanical stability of these thin 33.4YSZ layers were also observed by the wear test (Table 3). Our results show that the wear rate decreased

Table 3: Wear rate of 33.4YSZ coated and uncoated steel.

Sample	Wear rate ($\times 10^{-5}$ g/Nm)
Uncoated	2.2 ± 0.1
1 layer	2.1 ± 0.3
2 layers	1.9 ± 0.1
3 layers	1.3 ± 0.2

41% from 2.2×10^{-5} g/Nm down to 1.3×10^{-5} g/Nm for steel and three layers of YSZ, respectively. These values are similar to those reported for plasma sprayed calcia and magnesia zirconia coatings, which range between 0.6 and 6.25×10^{-5} g/Nm [52], and slightly higher than other YSZ coatings, with values of 0.14×10^{-6} g/Nm [53]. Although in less concentration, EDS elemental maps (see Figure S2 in the supplementary material) showed that zirconia was still present on the surface of steel after the wear test, most likely as the result of the good adherence and higher hardness achieved. Contrary to previous results, the wear rate did not decrease with a higher number of layers [23]. This could be related to the extended sintering time of 48 hours, which promoted the densification and the formation of more crystalline films [17, 26].

4. Conclusions

Our work stressed the importance of controlling extraction rates and sintering time during the deposition of YSZ coatings through sol-gel dip-coating. In particular, faster extraction rates of 0.67 mm s^{-1} deposited toward the viscous drag regime were needed to achieve uniform coating without apparent surface cracks. This was possibly related to variations in the adhesion and capillary pressure of the solvent on the surface of YSZ compared with steel. We also observed that at 700°C, it was possible to achieve the thermodynamically stable cubic phase, only after heat treatments of 48 hours, as confirmed by Raman spectroscopy. Moreover, the prolonged heat treatment times improved the mechanical properties of the coatings produced since hardness increased to approximately twice the value of steel (from 1.18 to 2.28 GPa). Additionally, the deposition and densification of YSZ coatings resulted in a decrease of 41% in the wear rate. We demonstrated that for low sintering temperatures, such as 700°C, 33.4 mol% yttria and 48 hours of heat treatment are needed to achieve maximum crystallinity and cubic phase.

Data Availability

The data used to support the findings of this study are available from the corresponding author upon request.

Disclosure

This manuscript has been authored by UT-Battelle, LLC, under contract DE-AC05-00OR22725 with the US Department of Energy (DOE). The US government retains, and the publisher, by accepting the article for publication, acknowledges that the US government retains a nonexclusive, paid-up, irrevocable, worldwide license to publish or reproduce the published form of this manuscript or allow others to do so, for US government purposes. DOE will provide public access to these results of federally sponsored research in accordance with the DOE Public Access Plan (http://energy.gov/downloads/doe-public-access-plan).

Conflicts of Interest

The authors declare that they have no known competing financial interests or personal relationships that could have appeared to influence the work reported in this paper.

Acknowledgments

This material is based upon work supported by a grant from CONACYT (project number: 245629, CONACYT-Horizon2020) and forms part of the European project SAMOFAR (A Paradigm Shift in Reactor Safety with the Molten Salt Fast Reactor). The authors would like to acknowledge CONACYT for the MSc and Ph.D. grants awarded to F. J. Cano, O. Castilleja-Escobedo, L. J. Espinoza-Pérez, and C. Reynosa-Martínez.

Supplementary Materials

Figure S1: TGA curve of YSZ with 33.4 mol% $YO_{1.5}$ (33.4YSZ). Figure S2: EDS elemental maps showing that zirconia was still present on the surface of steel after the wear test. *(Supplementary Materials)*

References

[1] J. Wu, J. Chen, X. Kang et al., "A novel concept for a molten salt reactor moderated by heavy water," *Annals of Nuclear Energy*, vol. 132, pp. 391–403, 2019.

[2] A. R. Shankar, K. Thyagarajan, and U. K. Mudali, "Corrosion behavior of candidate materials in molten LiCl-KCl salt under argon atmosphere," *Corrosion*, vol. 69, no. 7, pp. 655–665, 2013.

[3] V. Firouzdor, J. Brechtl, L. Wilson, B. Semerau, K. Sridharan, and T. R. Allen, "Development of yttrium stabilized zirconia (YSZ) diffusion barrier coatings for mitigation of fuel-cladding chemical interactions," *Journal of Nuclear Materials*, vol. 438, no. 1-3, pp. 268–277, 2013.

[4] P. K. Shukla, E. Hemanth Rao, E. Vetrivendan et al., "Evaluation of plasma sprayed sacrificial thermal barrier coatings for core catcher of future sodium cooled fast reactors," *Annals of Nuclear Energy*, vol. 107, pp. 31–36, 2017.

[5] T. Dharini, P. Kuppusami, P. Panda, R. Ramaseshan, and A. M. K. Kirubaharan, "Nanomechanical behaviour of Ni - YSZ nanocomposite coatings on superalloy 690 as diffusion barrier coatings for nuclear applications," *Ceramics International*, vol. 46, no. 15, pp. 24183–24193, 2020.

[6] L. J. Espinoza-Pérez, E. López-Honorato, and L. A. González, "Development of ZrO_2 and YSZ coatings deposited by PE-CVD below 800 °C for the protection of Ni alloys," *Ceramics International*, vol. 46, no. 10, pp. 15621–15630, 2020.

[7] K. Mo, G. Lovicu, X. Chen, H. M. Tung, J. B. Hansen, and J. F. Stubbins, "Mechanism of plastic deformation of a Ni-based superalloy for VHTR applications," *Journal of Nuclear Materials*, vol. 441, no. 1-3, pp. 695–703, 2013.

[8] B. A. Thiele, F. Schubert, H. Derz, and G. Pott, "Influence of test temperature on post irradiation, high temperature tensile and creep properties of X8 CrNiMoNb 1616, X10 NiCrAlTi 32 20 (Alloy 800) and $NiCr_{22}Fe_{18}Mo$ (Hastelloy X)," *Journal of Nuclear Materials*, vol. 171, no. 1, pp. 94–102, 1990.

[9] D. S. Aidhy, Y. Zhang, and W. J. Weber, "Radiation damage in cubic ZrO_2 and yttria-stabilized zirconia from molecular dynamics simulations," *Scripta Materialia*, vol. 98, pp. 16–19, 2015.

[10] J. M. Costantini, F. Beuneu, and W. J. Weber, "Radiation damage in cubic-stabilized zirconia," *Journal of Nuclear Materials*, vol. 440, no. 1-3, pp. 508–514, 2013.

[11] K. E. Sickafus, H. Matzke, T. Hartmann et al., "Radiation damage effects in zirconia," *Journal of Nuclear Materials*, vol. 274, no. 1-2, pp. 66–77, 1999.

[12] A. Debelle, S. Moll, B. Décamps et al., "Ability of cubic zirconia to accommodate radiation damage," *Scripta Materialia*, vol. 63, no. 6, pp. 665–668, 2010.

[13] P. Stefanov, D. Stoychev, I. Valov, A. Kakanakova-Georgieva, and T. Marinova, "Electrochemical deposition of thin zirconia films on stainless steel 316 L," *Materials Chemistry and Physics*, vol. 65, no. 2, pp. 222–225, 2000.

[14] Y. Pan, J. H. Zhu, M. Z. Hu, and E. A. Payzant, "Processing of YSZ thin films on dense and porous substrates," *Surface and Coatings Technology*, vol. 200, no. 5-6, pp. 1242–1247, 2005.

[15] P. Lenormand, D. Caravaca, C. Laberty-Robert, and F. Ansart, "Thick films of YSZ electrolytes by dip-coating process," *Journal of the European Ceramic Society*, vol. 25, no. 12, pp. 2643–2646, 2005.

[16] C. Viazzi, J. P. Bonino, and F. Ansart, "Synthesis by sol-gel route and characterization of yttria stabilized zirconia coatings for thermal barrier applications," *Surface and Coatings Technology*, vol. 201, no. 7, pp. 3889–3893, 2006.

[17] M. A. Domínguez-Crespo, A. García-Murillo, A. M. Torres-Huerta, F. J. Carrillo-Romo, E. Onofre-Bustamante, and C. Yáñez-Zamora, "Characterization of ceramic sol-gel coatings as an alternative chemical conversion treatment on commercial carbon steel," *Electrochimica Acta*, vol. 54, no. 10, pp. 2932–2940, 2009.

[18] A. Zarkov, A. Stanulis, J. Sakaliuniene et al., "On the synthesis of yttria-stabilized zirconia: a comparative study," *Journal of Sol-Gel Science and Technology*, vol. 76, no. 2, pp. 309–319, 2015.

[19] S. Rezaee, G. R. Rashed, and M. A. Golozar, "Electrochemical and oxidation behavior of yttria stabilized zirconia coating on zircaloy-4 synthesized via sol-gel process," *International Journal of Corrosion*, vol. 2013, 9 pages, 2013.

[20] R. L. Winter, P. Singh, M. K. King, M. K. Mahapatra, and U. Sampathkumaran, "Protective ceramic coatings for solid oxide fuel cell (SOFC) balance-of-plant components," *Advances in Materials Science and Engineering*, vol. 2018, Article ID 9121462, 17 pages, 2018.

[21] C. Viazzi, A. Deboni, J. Zoppas Ferreira, J. P. Bonino, and F. Ansart, "Synthesis of yttria stabilized zirconia by sol-gel route: influence of experimental parameters and large scale production," *Solid State Sciences*, vol. 8, no. 9, pp. 1023–1028, 2006.

[22] J. Sniezewski, Y. LeMaoult, P. Lours et al., "Sol-gel thermal barrier coatings: optimization of the manufacturing route and durability under cyclic oxidation," *Surface and Coatings Technology*, vol. 205, no. 5, pp. 1256–1261, 2010.

[23] W. Zhang, G. Ji, A. Bu, and B. Zhang, "Corrosion and tribological behavior of ZrO2Films prepared on stainless steel surface by the sol-gel method," *ACS Applied Materials & Interfaces*, vol. 7, no. 51, pp. 28264–28272, 2015.

[24] M. Yashima, M. Kakihana, and M. Yoshimura, "Metastable-stable phase diagrams in the zirconia-containing systems utilized in solid-oxide fuel cell application," *Solid State Ionics*, vol. 86-88, pp. 1131–1149, 1996.

[25] J. Fenech, C. Viazzi, J. P. Bonino, F. Ansart, and A. Barnabé, "Morphology and structure of YSZ powders: comparison between xerogel and aerogel," *Ceramics International*, vol. 35, no. 8, pp. 3427–3433, 2009.

[26] S. K. Tiwari, J. Adhikary, T. B. Singh, and R. Singh, "Preparation and characterization of sol-gel derived yttria doped zirconia coatings on AISI 316L," *Thin Solid Films*, vol. 517, no. 16, pp. 4502–4508, 2009.

[27] W. Liu, Y. Chen, C. Ye, and P. Zhang, "Preparation and characterization of doped sol-gel zirconia films," *Ceramics International*, vol. 28, no. 4, pp. 349–354, 2002.

[28] E. Courtin, P. Boy, C. Rouhet et al., "Optimized sol-gel routes to synthesize yttria-stabilized zirconia thin films as solid electrolytes for solid oxide fuel cells," *Chemistry of Materials*, vol. 24, no. 23, pp. 4540–4548, 2012.

[29] S. G. Kim, S. W. Nam, S. P. Yoon et al., "Sol-gel processing of yttria-stabilized zirconia films derived from the zirconium n-butoxide-acetic acid-nitric acid-water-isopropanol system," *Journal of Materials Science*, vol. 39, no. 8, pp. 2683–2688, 2004.

[30] M. T. Soo, N. Prastomo, A. Matsuda et al., "Elaboration and characterization of sol-gel derived ZrO_2 thin films treated with hot water," *Applied Surface Science*, vol. 258, no. 13, pp. 5250–5258, 2012.

[31] R. Shoja Razavi and M. R. Loghman-Estarki, "Advance techniques for the synthesis of nanostructured zirconia-based ceramics for thermal barrier application," in *Sol-gel Based Nanoceramic Materials: Preparation, Properties and Applications*, A. Mishra, Ed., Springer, Cham, 2016.

[32] D. R. Clarke and S. R. Phillpot, "Thermal barrier coating materials," *Materials Today*, vol. 8, no. 6, pp. 22–29, 2005.

[33] C. W. Kuo, Y. H. Lee, K. Z. Fung, and M. C. Wang, "Effect of Y_2O_3 addition on the phase transition and growth of YSZ nanocrystallites prepared by a sol-gel process," *Journal of Non-Crystalline Solids*, vol. 351, no. 4, pp. 304–311, 2005.

[34] D. D. Upadhyaya, M. R. Gonal, and R. Prasad, "Studies on crystallization behaviour of 3Y-TZP/Al_2O_3 composite powders," *Materials Science and Engineering A*, vol. 270, no. 2, pp. 133–136, 1999.

[35] S. Gutzov, J. Ponahlo, C. L. Lengauer, and A. Beran, "Phase characterization of precipitated Zirconia," *Journal of the American Ceramic Society*, vol. 77, no. 6, pp. 1649–1652, 1994.

[36] R. C. Garvie, "The occurrence of metastable tetragonal zirconia as a crystallite size effect," *The Journal of Physical Chemistry*, vol. 69, no. 4, pp. 1238–1243, 1965.

[37] R. Srinivasan, R. J. De Angelis, G. Ice, and B. H. Davis, "Identification of tetragonal and cubic structures of zirconia using synchrotron x-radiation source," *Journal of Materials Research*, vol. 6, no. 6, pp. 1287–1292, 1991.

[38] C. Viazzi, J. P. Bonino, F. Ansart, and A. Barnabé, "Structural study of metastable tetragonal YSZ powders produced via a sol-gel route," *Journal of Alloys and Compounds*, vol. 452, no. 2, pp. 377–383, 2008.

[39] H. G. Scott, "Phase relationships in the zirconia-yttria system," *Journal of Materials Science*, vol. 10, no. 9, pp. 1527–1535, 1975.

[40] A. Feinberg and C. H. Perry, "Structural disorder and phase transitions in ZrO_2-Y_2O_3 system," *Journal of Physics and Chemistry of Solids*, vol. 42, no. 6, pp. 513–518, 1981.

[41] M. Yashima, K. Ohtake, M. Kakihana, H. Arashi, and M. Yoshimura, "Determination of tetragonal-cubic phase boundary of Zr1−XRXO2−X2 (R = Nd, Sm, Y, Er and Yb) BY Raman scattering," *Journal of Physics and Chemistry of Solids*, vol. 57, no. 1, pp. 17–24, 1996.

[42] Y. Hemberger, N. Wichtner, C. Berthold, and K. G. Nickel, "Quantification of yttria in stabilized zirconia by Raman spectroscopy," *International Journal of Applied Ceramic Technology*, vol. 13, no. 1, pp. 116–124, 2016.

[43] I. Bačić, H. Otmačić Ćurković, L. Ćurković, V. Mandić, and Z. Šokčević, "Corrosion protection of AISI 316L stainless steel with the Sol- Gel yttria stabilized ZrO_2 films: effects of sintering temperature and doping," *International Journal of Electrochemical Science*, vol. 11, no. 11, pp. 9192–9205, 2016.

[44] M. Faustini, B. Louis, P. A. Albouy, M. Kuemmel, and D. Grosso, "Preparation of sol-gel films by dip-coating in extreme conditions," *Journal of Physical Chemistry C*, vol. 114, no. 17, pp. 7637–7645, 2010.

[45] C. J. Brinker, G. C. Frye, A. J. Hurd, and C. S. Ashley, "Fundamentals of sol-gel dip coating," *Thin Solid Films*, vol. 201, no. 1, pp. 97–108, 1991.

[46] Z. E. Sánchez-Hernández, M. A. Domínguez-Crespo, A. M. Torres-Huerta, E. Onofre-Bustamante, J. Andraca Adame, and H. Dorantes-Rosales, "Improvement of adhesion and barrier properties of biomedical stainless steel by deposition of YSZ coatings using RF magnetron sputtering," *Materials Characterization*, vol. 91, pp. 50–57, 2014.

[47] R. Ghasemi and H. Vakilifard, "Plasma-sprayed nanostructured YSZ thermal barrier coatings: thermal insulation capability and adhesion strength," *Ceramics International*, vol. 43, no. 12, pp. 8556–8563, 2017.

[48] J. Wang, J. Sun, H. Zhang et al., "Effect of spraying power on microstructure and property of nanostructured YSZ thermal barrier coatings," *Journal of Alloys and Compounds*, vol. 730, pp. 471–482, 2018.

[49] R. Vert, P. Carles, E. Laborde, G. Mariaux, E. Meillot, and A. Vardelle, "Adhesion of ceramic coating on thin and smooth metal substrate: a novel approach with a nanostructured ceramic interlayer," *Journal of Thermal Spray Technology*, vol. 21, no. 6, pp. 1128–1134, 2012.

[50] M. J. Filiaggi, R. M. Pilliar, and D. Abdulla, "Evaluating sol-gel ceramic thin films for metal implant applications. II. Adhesion and fatigue properties of zirconia films on Ti-6Al-4V," *Journal of Biomedical Materials Research*, vol. 33, no. 4, pp. 239–256, 1996.

[51] S. K. Tiwari, M. Tripathi, and R. Singh, "Electrochemical behavior of zirconia based coatings on mild steel prepared by sol-gel method," *Corrosion Science*, vol. 63, pp. 334–341, 2012.

[52] M. A. E. Hafez, S. A. Akila, M. A. Khedr, and A. S. Khalil, "Improving wear resistance of plasma-sprayed calcia and magnesia-stabilized zirconia mixed coating: roles of phase stability and microstructure," *Scientific Reports*, vol. 10, no. 1, article 78088, 2020.

[53] D. Kumar and K. N. Pandey, "Experimental investigations of sol-gel process parameters for wear reduction on thermal barrier coated AA2024 aluminum alloys with the use of Taguchi-based optimization," *Sādhanā*, vol. 45, no. 1, 2020.